Stem Cell Research 92 (2026) 103937

Contents lists available at ScienceDirect

Stem Cell Research

journal homepage: www.elsevier.com/locate/scr

Lab Resource: Genetically-Modified Single Cell Line

Generation of human induced pluripotent stem cell lines carrying a heterozygous and homozygous *PRKD1* c.1774G > A genetic variant causing syndromic congenital defects

Fabian Witthoff [a,b], Niels Pietsch [a,b], Philipp Henning [c], Leah S. Meier [a,b], Sigrid Fuchs [d], Christa Augustin [e], Julia Orth [a,b], Konstantina Stathopoulou [a,b], Ellen Orthey [a], Elisabeth Krämer [a], Lucie Carrier [a,b], Friedrich W. Herberg [c], Nadine Spielmann [f], Marc-Philip Hitz [g], J. David Brook [h], Siobhan Loughna [h], Friederike Cuello [a,b,*]

[a] Institute of Experimental Pharmacology and Toxicology, University Medical Center Hamburg-Eppendorf, Hamburg, Germany
[b] DZHK (German Center for Cardiovascular Research), Partner Site North, University Medical Center Hamburg-Eppendorf, Hamburg, Germany
[c] Institute of Biochemistry, University Kassel, Kassel, Germany
[d] Institute of Human Genetics, University Medical Center Hamburg-Eppendorf, Hamburg, Germany
[e] Institute of Legal Medicine, Forensic Genetics, University Medical Center Hamburg-Eppendorf, Hamburg, Germany
[f] Institute of Experimental Genetics, Helmholtz Center Munich, Munich, Germany
[g] University Institute of Human Genetics, University Oldenburg, Oldenburg, Germany
[h] School of Life Sciences, University of Nottingham, Nottingham, UK

A B S T R A C T

Protein kinase D1 (PRKD1) is a serine threonine kinase with roles in the regulation of embryonic development, contractility, vesicle transport and cytoskeleton organization. Consequently, variants in *PRKD1* that alter its kinase activity are associated with severe anomalies, manifesting as syndromic congenital defects in patients. To investigate the molecular pathomechanisms underlying *PRKD1* genetic variants, the patient-derived *PRKD1* p.G592R (c.1774 G > A) mutation was introduced in heterozygous and homozygous configuration into the human induced pluripotent stem cell line (AICS-0031-035:WTC-mTagRFPT-TUBA1B) with CRISPR/Cas9 technology and were thoroughly validated. These hiPSC lines constitute a valuable platform for dissecting the molecular consequences of impaired PRKD1 signaling.

Resource Table

Unique stem cell line identifier	hiPSC-line 1 (heterozygous): **UCSFi001-A-1T** hiPSC-line 2 (homozygous): **UCSFi001-A-1U**
Alternative name(s) of stem cell line	hiPSC-line 1 (heterozygous): **PRKD1-G592R-het** hiPSC-line 2 (homozygous): **PRKD1-G592R-hom**
Institution	Institute of Experimental Pharmacology and Toxicology, University Medical Center Hamburg-Eppendorf, Hamburg, Germany
Contact information of the reported cell line distributor	Friederike Cuello (f.cuello@uke.de); Institute of Experimental Pharmacology and Toxicology; University Medical Center Hamburg-Eppendorf, Martinistrasse 52; 20,246 Hamburg, Germany. Tel.: +49 (0) 40/7410 57204; Fax: +49(0) 40/7410–54876
Type of cell line	iPSC
Origin	human
Additional origin info	Age: 30–34 male Ethnicity: Asian
Cell Source	Dermal fibroblasts
Method of reprogramming	Non-integrating episomal vectors
Clonality	Clonal
Evidence of the reprogramming transgene loss (including genomic copy if applicable)	No vector detectable in RT-qPCR

(*continued on next column*)

Resource Table (*continued*)

(*continued on next page*)

* Corresponding author at: Institute of Experimental Pharmacology and Toxicology, University Medical Center Hamburg-Eppendorf, Hamburg, Germany.
E-mail address: f.cuello@uke.de (F. Cuello).

https://doi.org/10.1016/j.scr.2026.103937
Received 21 December 2025; Received in revised form 12 February 2026; Accepted 14 February 2026
Available online 16 February 2026

Resource Table (*continued*)

The cell culture system used	Matrigel®/Geltrex™, mTeSR™ plus, CloneR™ FTDA for maintenance hiPSC culture (37C, 5% CO_2, 5% O_2)
Type of the Genetic Modification	Missense genetic variant, *PRKD1* c.1774 G > A (p.G592R)
Associated disease	Variant is associated with syndromic congenital heart disease
Gene/locus modified in the reported transgenic line	*PRKD1* c.1774G > A (p.G592R, p.Gly592Arg), chromosome 14q12
Method of modification / user-customisable nucleases (UCN) used, the resource used for design optimisation	CRISPR/Cas9, IDT
User-customisable nuclease (UCN) delivery method	Nucleofection of RNP complex (crRNA, tracrRNA and Cas9)
All double-stranded DNA genetic material molecules introduced into the cells	None
Evidence of the absence of random integration of any plasmids or DS DNA introduced into the cells.	Sanger sequencing and PCR
Analysis of the nuclease-targeted allele status	Sanger sequencing and PCR
Homozygous allele status validation	verified
Method of the off-target nuclease activity prediction and surveillance	Targeted PCR and Sanger sequencing of the top 10 off-target loci determined by the cfd off-target score
Descriptive name of the transgene	N/A
Eukaryotic selective agent resistance cassettes (including inducible, gene/cell type-specific)	N/A
Inducible/constitutive expression system details	None; the parental hiPSC line expresses RFP-TUBA1B in monogenic form
Date archived/stock creation date	PRKD1-G592R-het (clone A2): MCB 20.09.2021; passage 38 PRKD1-G592R-hom (clone E8): MCB 21.10.2021; passage 42
Cell line repository/bank	hPSCreg.eu
Ethical/GMO work approvals	University of California San Francisco, 10–02521
Addgene/public access repository recombinant DNA sources' disclaimers (if applicable)	N/A

1. Resource utility

Generation of human induced pluripotent stem cell (hiPSC) lines carrying the patient PRKD1-G592R-variant enables investigation of the molecular consequences of disturbed kinase signalling leading to human disease. These lines represent an invaluable, ethically sustainable and potentially inexhaustible resource particularly in the light of embryonic lethality observed in humanized mouse models.

2. Resource Details

With a prevalence of 9 per 1000 live births, congenital heart disease (CHD) remains the leading cause of mortality in children under one year of age. While most genetic variants associated with CHD affect genes encoding sarcomeric proteins, pathogenic variants in protein kinase genes have only recently begun to receive attention.

Exome sequencing of patients with syndromic and non-syndromic CHD identified a *de novo* missense variant p.G592R (c.1774 G > A) in *PRKD1*, the gene encoding protein kinase D1 (PRKD1) (Sifrim et al. 2016). The PRKD kinase family comprises three highly homologous isoforms that are activated upon diacylglycerol-binding and protein kinase C-mediated phosphorylation (Avkiran et al. 2008). PRKD1 activation regulates a broad spectrum of cellular processes, including embryonic development (Waheed-Ullah et al. 2024), cargo transport (Malhotra and Campelo 2011), myocyte enhancer factor-dependent transcription (Fielitz et al. 2008), among others. To date, only pathogenic variants in *PRKD1* have been causally linked to CHD (Steinberg 2021).

More recently, a case report described early onset pulmonary valve stenosis, tooth loss, advanced bone ageing and widespread teleangiectasia in a patient carrying the PRKD1 p.G592R mutation (Alter et al. 2021). Functional analysis demonstrated that recombinant PRKD1 p.G592R retains lipid-dependent autocatalytic activity, but exhibits markedly reduced activity towards its substrates. Given that global *Prkd1*-targeted knockout mice are embryonically lethal, these findings underscore the urgent need for a human disease model.

The p.G592R (c.1774 G > A) variant is located within a highly conserved kinase domain of PRKD1, specifically in the glycine-rich loop (Fig. 1A**;** red). This structural element is essential for proper ATP-binding, which is stabilized and correctly orientated by a lysine residue in position 612. Substitution of the small glycine at position 592 by a larger, polar arginine is therefore predicted to disrupt ATP-binding and to impair kinase activity (Fig. 1A**;** p.G592R).

With CRISPR/Cas9 genome editing, the patient-derived missense variant PRKD1-p.G592R (c.1774 G > A) was introduced in heterozygous and homozygous configurations into a hiPSC line expressing an RFP-tagged α1b tubulin. This cell model enables investigation of the pathophysiological consequences of the variant and facilitates analysis of the interplay between mutant PRKD1 and the *trans*-Golgi-network.

With the repair template T1 a point mutation was introduced in position c.1774 G > A to generate the patient-specific mutation p.G592R. With this, a novel Xba1 restriction site enabling early detection of positive clones is created. Furthermore, the point mutation c. 1779 G > A was introduced to prevent the ribonucleoprotein from binding to already edited DNA strands. As conventional PAM silencing was not possible without altering the resulting amino acid composition, recutting of the DNA was attenuated by altering the nucleotides of the seeding region at position 13 and 18 (Fig. 1B) (Anderson et al. 2015). Following the harvest of gDNA from all clones a XbaI digest of the PCR product was performed, with the isogenic control showing the expected band of 885 bp, heterozygous clones three bands of 885, 577 and 288 bp and homozygous clones two bands of 577 and 288 bp (Fig. 1C). To further confirm the genome editing outcome, we performed Sanger sequencing around the PAM site, which confirmed the correct mutation in position c.1774 G > A in heterozygous and homozygous form (Fig. 1D).

Subsequently, we compared essential hiPSC characteristics of the generated lines. Both exhibited an intact karyotype confirmed by two independent methods (Fig. 1E**; Supplementary Fig. 1A**). Finally, to ensure the CRISPR-Cas9 editing was specific to the *PRKD1* locus, we sequenced the top ten most likely off-target sites for each line. No alterations were detected in any of the loci in PRKD1-G592R-het (**UCSFi001-A-1T**) and PRKD1-G592R-hom (**UCSFi001-A-1U**), confirming the specificity of our approach and ruling out off-target effects (**Supplementary Fig. 1B**). HiPSCs maintained a normal morphology (**Supplementary Fig. 1C**).

Authentication of both hiPSC-lines was ascertained by short tandem repeat (STR) analysis (**Supplementary Table 2**). Mycoplasma contamination was ruled out (Fig. 1F) and flow cytometry revealed a high pluripotency value of 96.6% (Fig. 1G**;** het; upper panel) and 99.7% (Fig. 1G**;** hom; bottom panel) for Stage-specific Embryonic Antigen-3 (SSEA-3).

To further validate pluripotency, we differentiated the cells into mesodermal, endodermal and ectodermal lineages. Immunofluorescence analysis for the presence of key marker genes (Brachyury, NCAM-1 for mesoderm; HNF 3b, SOX17 for endoderm; NESTIN, PAX 6 for ectoderm; Fig. 1H) was performed. Additionally, both, heterozygous and homozygous hiPSCs, were differentiated into hiPSC-cardiomyocytes to assess mesodermal differentiation potential. This was confirmed by the presence of 30—80% cardiac troponin T (cTnT)-positive cells (n = 2–4 independent differentiation runs; Fig. 1I).

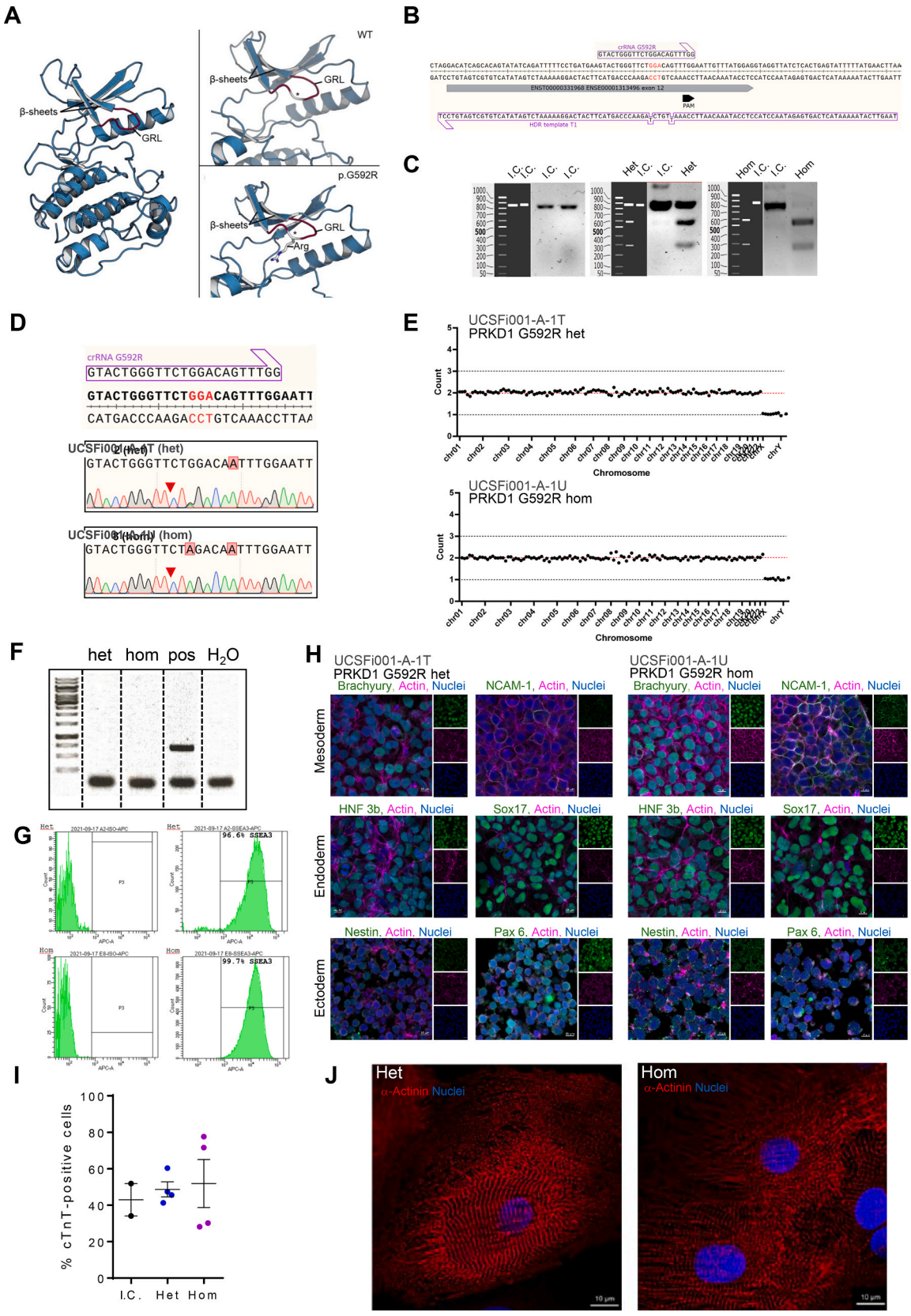

Fig. 1. Generation and validation of a heterozygous (het) and homozygous (hom) patient-specific PRKD1 p.G592R mutation in human-induced pluripotent stem cell-derived cardiomyocytes. The term "I.C." refers to the isogenic control and the term "pos" refers to positive control.

Additionally, we analyzed the morphology of heterozygous and homozygous hiPSC-cardiomyocytes by immunofluorescence imaging with an anti-α-actinin antibody (red) that stains the Z-discs and DAPI (blue) for the nuclei. This revealed regular myofilament morphology for both lines (Fig. 1J).

3. Materials and methods

3.1. Human-induced pluripotent stem cells

The hiPSC line AICS-0031–035, derived from the parental line UCSFi001-A is registered in hPSCreg and was purchased from https://www.allencell.org/cell-catalog.html.

3.2. Genome editing with CRISPR/Cas9

PRKD1-G592R-het (**UCSFi001-A-1T**) and PRKD1-G592R-hom (**UCSFi001-A-1U**) hiPSC-lines were generated using CRISPR/Cas9 with a crRNA targeting the location of interest with a symmetric homology-directed repair template that was designed complementary to the target strand consisting of 106 nucleotides including two mismatches (CRISPOR.org; IDT tools; Fig. 1B; Tables 1 and 2). The resulting missense variant induces an Gly/Arg amino acid exchange. The crRNA, tracrRNA and a ssODN were co-nucleofected into hiPSCs (AICS-0031–035; passage 29) using the Amaxa 4D-Nucleofector™ (Program: CA137, Lonza). Homology-directed repair (HDR) was induced by providing a ssODN utilized as a HDR template. Cells were seeded in mTeSR+™ with CloneR™ (1:10 in mTeSR+™) on Matrigel® (1:60 in RPMI)-coated 12-well plates and redistributed at low density with 10 μM

Table 1
Characterization and validation.

Classification	Output type	Result	Data
Schematic of a transgene/genetic modification	Schematic illustrating the structure and location of the introduced genetic modification	Localisation of the mutation in the kinase structure and in the sequence analysis	Fig. 1 **panel A,B**
Morphology	Photography bright field	A visual record of the line's cellular morphology: typical pluripotent human stem cell morphology	**Supplementary Fig. 1 panel C**
Pluripotency status evidence for the described cell line	Qualitative analysis	Assess staining/expression of pluripotency markers: SSEA3	
	Quantitative analysis – Flow cytometry	>90% SSEA-3-positive cells	Fig. 1 **panel G**
Karyotype	G-banding, nCounter NanoString karyotyping panel for UCSFi001-A-1T; UCSFi001-A-1U	46XY	Fig. 1 **panel E; Supplementary Fig. 1 panel A**
Genotyping for the desired genomic alteration/allelic status of the gene of interest	PCR across the edited site or targeted allele-specific PCR	PCR / XbaI digest + Sanger sequencing	Fig. 1 **panel C, D**
	Evaluation of the – (homo-/ heterozygous status of introduced genomic alteration(s)	PCR / XbaI digest + Sanger sequencing	Fig. 1 **panel C, D**
	Transgene-specific PCR (when applicable)	N/A	N/A
Verification of the absence of random plasmid integration events	PCR/Southern	N/A	N/A
Parental and modified cell line genetic identity evidence	STR analysis, microsatellite PCR (mPCR) or specific (mutant) allele seq	Available for parental line. 29 allelic polymorphisms across 15 STR loci compared to donor fibroblasts	Data held by the provider.
		Fragment analysis: Genetic Analyzer SeqStudio™, GeneMapper –ID-X ®-Software (Thermo Fisher)	**Supplementary Table 2**
Mutagenesis / genetic modification outcome analysis	Sequencing (genomic DNA PCR or RT-PCR product)	Genomic DNA PCR and sequencing; Hetero- and homozygous	Fig. 1 **panel D**
Off-target nuclease activity analysis	PCR across top 10 predicted top likely off-target sites, whole genome/exome sequencing	Demonstration of the lack of NHEJ-caused mutagenesis in the top 10 predicted off-target Cas nuclease activity for the gRNA	**Supplementary Fig. 1 panel B**
Specific pathogen-free status	Mycoplasma	PCR negativity	Fig. 1 **panel F**
Multilineage differentiation potential	Directed differentiation; Expression of marker markers determined by RT-qPCR, flow cytometry or immunofluorescence	STEMdiff trilineage differentiation kit (ecto-, meso-, and endoderm) and cardiomyocyte differentiation (mesoderm); Flow cytometry: Mesodermal lineage, differentiation to cardiomyocytes – cardiac troponin T (cTnT) Immunofluorescence: Mesodermal lineage, differentiation to cardiomyocytes (α-actinin 2 and F-actin)	Fig. 1 **panel H**
List of recommended germ layer markers	Expression of these markers has to be demonstrated at mRNA (RT PCR) or protein (IF) levels, at least 2 markers need to be shown per germ layer	Ectoderm: NESTIN, PAX6 Endoderm: HNF3b, SOX17 Mesoderm: BRACHYURY, NCAM1, cTnT, α-actinin-2	IF and specific antibodies; Fig. 1 **panel H, J**
Outcomes of gene editing experiment (OPTIONAL)	Brief description of the outcomes in terms of clones generated/establishment approach/screening outcomes	ICE analysis: 16%	**Het:** 15/86 (17%) **Hom:** 4/86 (4,7%)
Donor screening (OPTIONAL)	HIV 1 + 2, Hepatitis B, Hepatitis C	N/A	N/A
Genotype – additional histocompatibility info (OPTIONAL)	Blood group genotyping	N/A	N/A
	HLA tissue typing	N/A	N/A

Table 2
Reagents details.

Antibodies and stains used for immunocytochemistry/flow-cytometry			
	Antibody	Dilution	Company Cat # and RRID
Pluripotency marker	Rat Anti-Human SSEA3 Antibody, PE Conjugated	1:80	BD Biosciences Cat# 560237, RRID: AB_1645542
	Rat IgM, k antibody	1:80	BD Biosciences Cat# 553943, RRID:AB_10056839
Differentiated cardiomyocyte marker	Cardiac Troponin T Antibody, anti-human/mouse/rat, REAfinity™	1:50	Miltenyi Biotec Cat# 130–119-674, RRID: AB_2751795
	REA Control Antibody (I), human IgG1, REAfinity™	1:50	Miltenyi Biotec Cat# 130–120-709, RRID: AB_2784399
Immunofluorescence	Anti-actinin-2 (2 h, RT)	1:500	Sigma Aldrich Cat# A7811, RRID: AB_476766
			R&D Systems, Biotechne:
	Anti-Nestin	1:62,5–1:20	Clone # 196908; MAB1259
	Anti-PAX6	1:40–1:13	AF8150
	Anti-HNF3b/FoxA2	1:40–1:13	AF2400
	Anti-SOX17	1:40–1:13	AF1924
	Anti-Brachyury	1:40–1:13	AF2085
	Anti-NCAM-1/CD56	1:40–1:13	AF2408
Dyes	DAPI	1 µg/mL	Sigma Cat# D9542
	AlexaFluor 633-Phalloidin/F-actin	1:100	Invitrogen Cat#A22284
Site-specific nuclease			
Nuclease information	Alt-R® S.p. Cas9	Nucl Nuclease 3NLS, 2 nmol, Cat# 1,081,058	
Delivery method	Nucleofection of RNP complex (crRNA, tracrRNA and Cas9)	Alt-R® CRISPR-Cas9 crRNA, 2 nmol (IDT®); Alt-R® CRISPR-Cas9 tracrRNA, ATTO™ 550, 5 nmol: Cat# 1,075,927 (IDT®)	
Selection/enrichment strategy	N/A		
Primers and Oligonucleotides used in this study			
	Target	**Forward/Reverse primer (5′-3′)**	
Targeted mutation analysis/sequencing	hPRKD1_CRISPR_fwd	TCCAAATAGCCATCTCAACAG	
	hPRKD1_CRISPR_rev	CCCTTTAACTGGCTGGAATC	
	hPrkd1_CRISPR_for2	ACCTCTGCCACTTAAGATCAGAAC	
	hPrkd1_CRISPR_rev2	AGTACTGTGTGTACAGTTTGCC	
Allele frequency qPCR		N/A	
crRNA sequence + PAM	crRNA G592R	GTACTGGGTTCTGGACAGTTTGG	
HDR template	HDR template 1	TAAGTTCATAAAAATACTCAGTGA GATAACCTACCTCCATAAACAAT TCCAAAtTGTCtAGAACCCAGTA CTTCATCAGGAAAAATCTGATAT ACTGTGCTGATGTCCT	
Top10 off-target (OT) mutagenesis predicted site sequencing primers	PRKD1_Offtarget1_fw	TGTGCATCAGTGTACCTTCTAGC	
	PRKD1_Offtarget1_rev	ACCTGGATTTCGGGTTGAG	
	PRKD1_Offtarget2_fw	AAGTGCCACCTTTCCCTCAG	
	PRKD1_Offtarget2_rev	TGATGCACTGTAGTGGGCAG	
	PRKD1_Offtarget3_fw	ACCCCTGTAGGGTTCTGTGA	
	PRKD1_Offtarget3_rev	CAGACCAAGATTGACTTTGGATAAC	
	PRKD1_Offtarget4_fw	CCTTCAACAAAGCATCTCTGC	
	PRKD1_Offtarget4_rev	TGCACCCAAGTATCATGTCC	
	PRKD1_Offtarget5_fw	CCACATTCTTCCGTGTTATGC	
	PRKD1_Offtarget5_rev	GGACTGGGATCTGGGCAGTTGGG	
	PRKD1_Offtarget6_fw	GTATTTGTGGCACTGTGAAGG	
	PRKD1_Offtarget6_rev	GCAACCTCCAGCATAAATGG	
	PRKD1_Offtarget7_fw	AAACGCTACAGCCTCTTTGG	
	PRKD1_Offtarget7_rev	GCCTGGGTTATTTCATTTGG	
	PRKD1_Offtarget8_fw	AGCCTCGGTCTCTGATGGTA	
	PRKD1_Offtarget8_rev	ACAACAGGCTGGACCTGAAC	
	PRKD1_Offtarget9_fw	AGAGCAGCTTTGGACAGAGG	
	PRKD1_Offtarget9_rev	TTTGGGAAATCCACTTAGCC	
	PRKD1_Offtarget10_fw	GCTGTCAATCTGGTCTCTGC	
	PRKD1_Offtarget10_rev	GACCATCAGAGCCTGCTACC	

Y-27632 to isolate single-cell clones. Colonies were manually picked, expanded in 48-well plates (37°C, 5% CO_2, 5% O_2), cryopreserved, and harvested for DNA extraction (Qiagen) and subsequent quality controls.

3.3. Validation of the PRKD1-G592R hiPSC-lines

By introducing the desired mutation, an XbaI-restriction was generated. From the isolated gDNA, a 885 bp PCR-amplicon was generated containing the mutation site. Following this, restriction enzyme digestion was performed allowing preselection of clones (Fig. 1C; Table 1). Clones showing the predicted restriction pattern were subsequently validated by PCR and Sanger sequencing (Fig. 1D; Table 1).

3.4. Karyotype and chromosome analysis

Karyotype analysis of the hiPSC lines was performed using the NanoString nCounter® Human Karyotype panel (Fig. 1E; Table 1), following the manufacturer's protocol. Complementary G-banding analysis of 15 metaphases from both lines confirmed an intact male karyotype (Supplementary Fig. 1A; Table 1). Authentication of the hiPSC-lines was ascertained by STR analysis (Supplementary Table 2; Table 1). For this, 1 ng of each sample was amplified with the PowerPlex® ESI Multiplex Kit (Promega) using 15 autosomal STR loci (D3S1358, TH01, D21S11, D18S51, D10S1248, D1S1656, D2S1338, D16S539, D22S1045, VWA, D8S1179, FGA, D2S441, D12S391, D19S391, SE33) and amelogenin for sex determination. Amplification was performed in a TPersonal 48Thermocycler (Biometra) according to the kit manufacturer's recommended protocol, using 28 cycles. Following amplification, fragment length analysis was performed on an SeqStudio Genetic Analyzer (ThermoFisher) using Internal Lane Standard WEN 500 (Promega). The resulting STR fragments were analysed with the GeneMapper® ID-X software.

3.5. Mycoplasma test

Mycoplasma testing of hiPSC-lines was performed by PCR according to previously established protocols (Shibamiya et al. 2020) (Fig. 1F; Table 1).

3.6. Flow cytometry analysis

Cells were suspended in PBS + 5% FCS for 15 min. After centrifugation the supernatant was discarded and cells were stained with the antibody for 30 min at 4°C. Flow cytometry was used to evaluate pluripotency and cardiomyocyte differentiation efficiency (anti-stage-specific embryonic antigen-3 (SSEA-3) and anti-troponin T (TNNT2)), respectively (Fig. 1G and I; Tables 1 and 2), in parallel with appropriate isotype controls. Data acquisition was performed using a FACS Canto II cytometer (BD Biosciences) at the UKE FACS Core Facility.

3.7. Pluripotency and lineage differentiation assessment

HiPSC pluripotency was confirmed using the STEMdiff™ Trilineage Differentiation Kit (Stemcell Technologies, #05230). Ectoderm, mesoderm and endoderm differentiation followed the manufacturer's protocol. Mesoderm induction was additionally achieved via cardiomyocyte monolayer differentiation (Mosqueira et al. 2018; Pietsch et al. 2024).

3.8. Immunostaining and confocal imaging

Cells were paraformaldehyde-fixed (4%; 10 min room-temperature), permeabilized (0.2% Triton X100/PBS; 20 min room-temperature), and stained (overnight 4C) for NESTIN and paired box 6 (PAX6; **ectoderm**); hepatocyte nuclear factor 3-beta (HNF3β) and SPRY-box transcription factor 17 (SOX17; **endoderm**); Brachyury, neural cell adhesion molecule 1 (NCAM1) and α-actinin (Fig. 1**H**, **J; mesoderm**). Immunofluorescence staining for α-actinin, along with F-actin by phalloidin and nuclei by DAPI (3 h at room-temperature). Imaging was performed using a Zeiss LSM 800 Airyscan confocal microscope.

Author contributions

FW, **NP** designed the CRISPR editing strategy. **FW** generated the hiPSC-lines. **PH, FWH** performed molecular modeling of PRKD1. **LSM** differentiated hiPSC-cardiomyocytes and performed immunofluorescence of 2D-hiPSC-cardiomyocytes. **SF** performed the chromosome analysis by Giemsa-banding, **CA** performed STR analysis; **JO** helped with hiPSC-culture and hiPSC-cardiomyocyte differentiation; **KS** supported data presentation; **EO** performed the trilineage differentiation and subsequent immunofluorescence; **EK** performed the karyotype analysis with the NanoString nCounter®; **LC** provided access to the isogenic control hiPSC-line; **NS**, **MPH**, **DJB**, **SL** represent the core PRKD1 research team, discussed data and provided patient information; **FC** conceptualized the hiPSC-line generation, analyzed data, wrote the manuscript and provided funding. All authors proofread the manuscript and provided critical comments on the scientific content.

CRediT authorship contribution statement

Fabian Witthoff: Methodology, Formal analysis, Data curation. **Niels Pietsch:** Conceptualization. **Philipp Henning:** Formal analysis. **Leah S. Meier:** Data curation. **Sigrid Fuchs:** Formal analysis, Data curation. **Christa Augustin:** Formal analysis, Data curation. **Julia Orth:** Formal analysis, Data curation. **Konstantina Stathopoulou:** Visualization. **Ellen Orthey:** Data curation. **Elisabeth Krämer:** Data curation. **Lucie Carrier:** Resources. **Friedrich W. Herberg:** Visualization. **Nadine Spielmann:** Resources. **Marc-Philip Hitz:** Resources. **J. David Brook:** . **Siobhan Loughna:** Resources. **Friederike Cuello:** Writing – review & editing, Writing – original draft, Supervision, Funding acquisition, Data curation, Conceptualization.

Declaration of competing interest

The authors declare that they have no known competing financial interests or personal relationships that could have appeared to influence the work reported in this paper.

Acknowledgements

The authors would like to gratefully acknowledge Prof. Dr. Thomas Eschenhagen, Institute of Experimental Pharmacology and Toxicology, Hamburg for providing the infrastructure allowing to perform this study. We would also like to thank Angelika Piasecki for help with hiPSC-culture and Jennifer Kaiser for help with the karyotyping as well as the UKE Cytometry und Cell Sorting Core Facility for providing the equipment to perform flow cytometry analysis. **FW** was supported by a medical graduate stipend of the DZHK. Parts of this work were subject of a medical doctorate at the medical faculty of the University of Hamburg.

Appendix A. Supplementary data

Supplementary data to this article can be found online at https://doi.org/10.1016/j.scr.2026.103937.

Data availability

No data was used for the research described in the article.

References

Alter, S., Zimmer, A.D., Park, M., Gong, J., Caliebe, A., Fölster-Holst, R., Torrelo, A., Colmenero, I., Steinberg, S.F., Fischer, J., 2021. Telangiectasia-ectodermal dysplasia-brachydactyly-cardiac anomaly syndrome is caused by de novo mutations in protein kinase D1. J. Med. Genet. 58, 415–421.

Anderson, E.M., Haupt, A., Schiel, J.A., Chou, E., Machado, H.B., Strezoska, Ž., Lenger, S., McClelland, S., Birmingham, A., Vermeulen, A., Smith, A.v., 2015. Systematic analysis of CRISPR-Cas9 mismatch tolerance reveals low levels of off-target activity. J. Biotechnol. 211, 56–65.

Avkiran, M., Rowland, A.J., Cuello, F., Haworth, R.S., 2008. Protein kinase d in the cardiovascular system: emerging roles in health and disease. Circ. Res. 102, 157–163.

Fielitz, J., Kim, M.S., Shelton, J.M., Qi, X., Hill, J.A., Richardson, J.A., Bassel-Duby, R., Olson, E.N., 2008. Requirement of protein kinase D1 for pathological cardiac remodeling. PNAS 105, 3059–3063.

Malhotra, V., Campelo, F., 2011. PKD regulates membrane fission to generate TGN to cell surface transport carriers. Cold Spring Harb. Perspect. Biol. 3.

Mosqueira, D., Mannhardt, I., Bhagwan, J.R., Lis-Slimak, K., Katili, P., Scott, E., Hassan, M., Prondzynski, M., Harmer, S.C., Tinker, A., Smith, J.G.W., Carrier, L., Williams, P.M., Gaffney, D., Eschenhagen, T., Hansen, A., Denning, C., 2018. CRISPR/Cas9 editing in human pluripotent stem cell-cardiomyocytes highlights arrhythmias, hypocontractility, and energy depletion as potential therapeutic targets for hypertrophic cardiomyopathy. Eur. Heart J. 39, 3879–3892.

Pietsch, N., Chen, C.Y., Kupsch, S., Bacmeister, L., Geertz, B., Herrera-Rivero, M., Siebels, B., Voß, H., Krämer, E., Braren, I., Westermann, D., Schlüter, H., Mearini, G., Schlossarek, S., van der Velden, J., Caporizzo, M.A., Lindner, D., Prosser, B.L., Carrier, L., 2024. Chronic activation of tubulin tyrosination improves heart function. Circ. Res. 135, 910–932.

Shibamiya, A., Schulze, E., Krauß, D., Augustin, C., Reinsch, M., Schulze, M.L., Steuck, S., Mearini, G., Mannhardt, I., Schulze, T., Klampe, B., Werner, T., Saleem, U., Knaust, A., Laufer, S.D., Neuber, C., Lemme, M., Behrens, C.S., Loos, M., Weinberger, F., Fuchs, S., Eschenhagen, T., Hansen, A., Ulmer, B.M., 2020. Cell banking of hiPSCs: a practical guide to cryopreservation and quality control in basic research. Curr. Protoc. Stem Cell Biol. 55, e127.

Sifrim, A., Hitz, M.P., Wilsdon, A., Breckpot, J., Turki, S.H., Thienpont, B., McRae, J., Fitzgerald, T.W., Singh, T., Swaminathan, G.J., Prigmore, E., Rajan, D., Abdul-Khaliq, H., Banka, S., Bauer, U.M., Bentham, J., Berger, F., Bhattacharya, S., Bu'Lock, F., Canham, N., Colgiu, I.G., Cosgrove, C., Cox, H., Daehnert, I., Daly, A., Danesh, J., Fryer, A., Gewillig, M., Hobson, E., Hoff, K., Homfray, T., Kahlert, A.K., Ketley, A., Kramer, H.H., Lachlan, K., Lampe, A.K., Louw, J.J., Manickara, A.K., Manase, D., McCarthy, K.P., Metcalfe, K., Moore, C., Newbury-Ecob, R., Omer, S.O., Ouwehand, W.H., Park, S.M., Parker, M.J., Pickardt, T., Pollard, M.O., Robert, L., Roberts, D.J., Sambrook, J., Setchfield, K., Stiller, B., Thornborough, C., Toka, O., Watkins, H., Williams, D., Wright, M., Mital, S., Daubeney, P.E., Keavney, B., Goodship, J., Abu-Sulaiman, R.M., Klaassen, S., Wright, C.F., Firth, H.V., Barrett, J. C., Devriendt, K., FitzPatrick, D.R., Brook, J.D., Hurles, M.E., 2016. Distinct genetic architectures for syndromic and nonsyndromic congenital heart defects identified by exome sequencing. Nat. Genet. 48, 1060–1065.

Steinberg, S.F., 2021. Decoding the Cardiac Actions of Protein Kinase D Isoforms. Mol. Pharmacol. 100, 558–567.

Waheed-Ullah, Q., Wilsdon, A., Abbad, A., Rochette, S., Bu'Lock, F., Hitz, M.P., Dombrowsky, G., Cuello, F., Brook, J.D., Loughna, S., 2024. Effect of deletion of the protein kinase PRKD1 on development of the mouse embryonic heart. J. Anat. 245, 70–83.